The effects of surface roughness, chloride, and molybdate on the corrosion behavior of iron in bicarbonate/carbonate solutions

Ahmed S. Alshamsi,* Afra G. AlBlooshi, Almaha S. Alshamsi, Asma Y. Alkaabi, Yasmeen S. Elnasiri and Mouza M. Aldhaheri

Department of Chemistry, College of Science, United Arab Emirates University (UAEU), Al Ain, UAE
**E-mail: a.alshamsi@uaeu.ac.ae*

Abstract

The effects of surface roughness, chloride ions, and molybdate ions on the corrosion behavior of pure iron was thoroughly investigated in bicarbonate/carbonate solutions at 22°C. Open circuit potential versus time, polarization resistance versus time, potentiodynamic polarization, electrochemical impedance spectroscopy (EIS), and scanning electron microscopy (SEM) were used for this investigation. The results demonstrated the presence of up to 2% molybdate ions does not enhance the corrosion resistance of pure iron in chloride-free bicarbonate/carbonate solutions. Moreover, molybdate ions and surface roughness have little effect on the passivity of iron in chloride-free bicarbonate/carbonate solutions. The effect of molybdate and surface roughness, however, changed in the presence of chloride. Iron with relatively smooth surface finish showed better corrosion resistance than iron with relatively rough surface finish. Moreover, the presence of molybdate improved the corrosion resistance of iron when chloride was present. The passive current densities decreased while the pitting potential increased in the presence of molybdate for both smooth and rough surface finish. SEM images taken after two days of immersion (at the open circuit potential) in chloride-containing solutions did not show any signs of pitting corrosion. SEM images taken after the polarization tests showed pitting corrosion in chloride-containing solutions in the absence of molybdate. Interestingly, SEM images taken after polarization did not show signs of pitting in chloride-containing solutions when 2% molybdate was present. The presence of molybdate enhanced the iron resistance to localized corrosion. Finally, the constant phase element can be treated as a non-ideal capacitor in chloride-free solutions for both the relatively smooth and relatively rough surface finish. In chloride-containing solutions, the constant phase element can be treated as a non-ideal capacitor for the relatively smooth surface finish, but not the relatively rough surface finish.

Keywords: *iron, corrosion, pitting, bicarbonate, carbonate, chloride, molybdate, electrochemical impedance spectroscopy, surface roughness, SEM.*

Received: September 18, 2019. Published: October 12, 2019 doi: 10.17675/2305-6894-2019-8-4-4

1. Introduction

Passivity and passivity breakdown of metals and alloys have been extensively reported in the literature. J. Soltis reviewed the passive film formation and breakdown in metallic materials including iron alloys [1]. Angathevar Veluchamy *et al.* published a critical review on the passive film formation and breakdown on iron electrode under different conditions including the effect of halides [2]. Reinforcing steel bars (rebars) can be exposed to carbonate, bicarbonate, and chloride [3]. Moreno *et al.* reported a minimum Cl^- concentration of 0.05% is required in order to induce passivity breakdown of reinforced steel in simulated concrete pore solution of bicarbonate/carbonate [3]. Yong Teck Tan *et al.* concluded that bicarbonate/carbonate ions have an inhibitive effect on the pitting corrosion of AISI 1020 carbon steel tested in saturated $Ca(OH)_2$ in the presence of chloride ions [4]. N.N. Andreev *et al.* concluded that the corrosion of reinforced steel occurs early in the course of steel hardening in chloride-containing concrete. Moreover, the growth rate of corrosion spots decreases significantly once the curing process is completed [5]. I.A. Gedvillo *et al.* concluded that steel is prone to pitting corrosion during the initial stage of concrete hardening with pitting corrosion intensified by the presence of chloride [6].

Molybdate ion (MoO_4^{2-}) has been gaining widespread acceptance as a non-toxic environmentally friendly inorganic corrosion inhibitor [7]. On the other hand, MoO_4^{2-} has been reported to increase the repassivation rate and to enhance resistance to localized corrosion [8–12]. In acidic chloride-containing solutions, the mechanism of inhibition by molybdate (MoO_4^{2-}) is thought to be a process of ion exchange, followed by the formation of an insoluble film reported to be ferric molybdate ($FeMoO_4$). The adsorption produces a layer that resists the corrosive effects to other anions, particularly chlorides and sulfates. The precipitate hinder the transpassive reaction leading to lower current densities [11]. Furthermore, relatively low MoO_4^{2-} concentrations were reported to decrease the corrosion resistance of various metals and alloys [8, 13–18]. Yong Teck Tan *et al.* reported that molybdate ions inhibited pitting corrosion of AISI 1020 carbon steel in Cl^--containing $Ca(OH)_2/NaHCO_3$ solutions [19]. It is worth mentioning that the tests were conducted under the open circuit potential conditions only.

Ilevbare and Burstein reported that the presence of MoO_4^{2-} affected both passivity and pit nucleation by deactivating the sites at which pit formation occurred and by reducing the pit size; consequently, becoming more difficult for pits to develop into stable ones [20].

Furthermore, corrosion behavior is influenced by surface roughness and texture [21]. Burstein and Pistorius reported that the nucleation rate of metastable pits of 304 stainless steel in solutions containing Cl^- ions increased with increasing surface roughness [22]. Wang *et al.* reported an increase in charge transfer resistance (R_{ct}) values with decreasing roughness for mild steel tested in ammonium chloride (NH_4Cl) solution [23]. Alshamsi and Alblooshi reported that the corrosion rate of Fe increased with increasing surface roughness in 0.1 M HCl and in 0.1 M H_2SO_4 [18].

The current work investigates the corrosion behavior of pure Fe in 0.3 M $NaHCO_3$ + 0.1 M Na_2CO_3. The solution simulates carbonated concrete [3]. Moreover, the effects of surface roughness, the presence of MoO_4^{2-} and the presence of Cl^- on the corrosion behavior are discussed.

The novelty of this work is in the use of pure Fe instead of carbon steel in carbonate/bicarbonate solutions. The use of pure iron instead of carbon steel minimizes the effect of inclusions on the passivity breakdown. Moreover, the current work examines the effect of MoO_4^{2-} as a corrosion inhibitor in the absence and presence of Cl^- ions using different surface roughness.

2. Experiments

Commercial Fe (99.99+ %) was tested in 0.3 M $NaHCO_3$ + 0.1 M Na_2CO_3 solutions in the absence and presence of MoO_4^{2-} and/or Cl^- at 22±1°C. An Fe rod, 2 mm in diameter, was coated with epoxy, but the cross-sectional area (0.0314 cm^2) was exposed to the testing solution. The sample was wet-ground using only grit paper P120 in order to maintain a relatively rough surface area. Alternatively, the sample was wet-ground using P120 followed by P320, P800, and finally with P1000 in order to maintain a relatively smooth surface area. The sample was cleaned with deionized water in ultrasound bath, washed with deionized water, and placed in a 3-electrode cell with platinum (Pt) as a counter-electrode and saturated Ag/AgCl electrode as the reference electrode. Two sets of experiments were conducted. In one set, the open circuit potential versus time (OCP *versus t*) was conducted first, followed by electrochemical impedance spectroscopy (*EIS*). In the other set, OCP *versus t* was conducted first, followed by the polarization resistance *versus* time (R_p *versus t*), and finally by the potentiodynamic polarization measurements. The OCP was monitored for one hour prior to each experiment upon the immersion in the solution. The R_p *versus t* measurements were conducted at a scanning rate of 0.1 mV s^{-1} with experiments conducted at ±20 mV *versus* the corrosion potential (E_c). Four data points were collected per R_p *versus t* experiment. EIS experiments were conducted using an applied alternating current (AC) potential of 10 mV with frequencies ranging from 0.005 to 100,000 Hz. The potentiodynamic polarization experiments were initiated at −250 mV *versus* the corrosion potential (E_c), scanned to +700 mV using a scanning rate of 1.0 mV s^{-1}. Magnetic stirring at a constant rate was maintained in all experiments. On average, three independent experiments were conducted for all specimens. Data were collected automatically with the aid of a potentiostat/galvanstat (Gamry G750). All data analyses and extrapolations were performed using Gamry corrosion software (Gamry Echem Analyst). The samples' surface morphologies were examined using scanning electron microscopy (SEM). The samples were cleaned in an ultrasound bath prior to SEM examination. Table 1 lists the solutions used in this study.

Table 1. Compositions of the solutions used in this study.

Solution	Composition
1	0.3 M $NaHCO_3$ + 0.1 M Na_2CO_3
2	0.3 M $NaHCO_3$ + 0.1 M Na_2CO_3 + 1% Na_2MoO_4
3	0.3 M $NaHCO_3$ + 0.1 M Na_2CO_3 + 2% Na_2MoO_4
4	0.3 M $NaHCO_3$ + 0.1 M Na_2CO_3 + 1% NaCl
5	0.3 M $NaHCO_3$ + 0.1 M Na_2CO_3 + 1% NaCl + 1% Na_2MoO_4
6	0.3 M $NaHCO_3$ + 0.1 M Na_2CO_3 + 1% NaCl + 2% Na_2MoO_4

3. Results and discussion

3.1. The corrosion behavior of Fe in the absence of Cl^- ions

Figure 1(a,b) provides SEM micrographs of the polished smooth (P1000) and the rough (P120) surface, respectively. Figure 2(a,b) shows the OCP *versus t* for Fe tested in 0.3 M $NaHCO_3$ + 0.1 M Na_2CO_3 as a function of MoO_4^{2-} and surface roughness. Figure 2a represents smooth surface finish (P1000) while Figure 2b represents rough surface finish (P120).

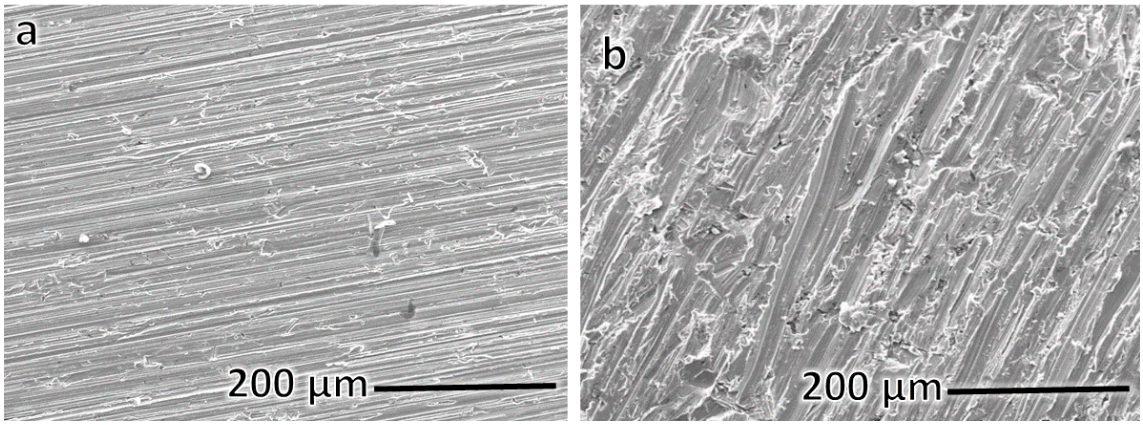

Figure 1. (a) SEM micrograph of polished Fe surface with *smooth* surface finish (P1000). **(b)** SEM micrograph of polished Fe surface with *rough* surface finish (P120).

All curves show steady increase in the OCP with time. Such steady increase in the OCP with time can be attributed to the transformation of pre-existing non-protective film to a stable protective one; the metal passivates in these solutions. Figure 3(a,b) shows R_p *versus t* curves with the average R_p values reported in Table 2a. Figure 4(a,b) shows the Nyquist plots for the smooth and rough surfaces, respectively. R_p and α values (Table 2b) were obtained by fitting the equivalent electrical circuit to the impedance data from the EIS measurements. Figure 5 shows the circuit used to fit the data. The R_p values in Table 2(a,b) show that the presence of MoO_4^{2-} resulted in little decrease in the R_p values for samples

with smooth surface finish (slightly higher corrosion rate). For the rough surface finish, the R_p values obtained from the R_p versus t experiments show little decrease in the presence of MoO_4^{2-} while the R_p values obtained from the EIS show no change in the presence of MoO_4^{2-}. Based on the above discussed results, the presence of MoO_4^{2-} does not enhance the corrosion resistance in these solutions. In fact, small concentration of MoO_4^{2-} might decrease the corrosion resistance.

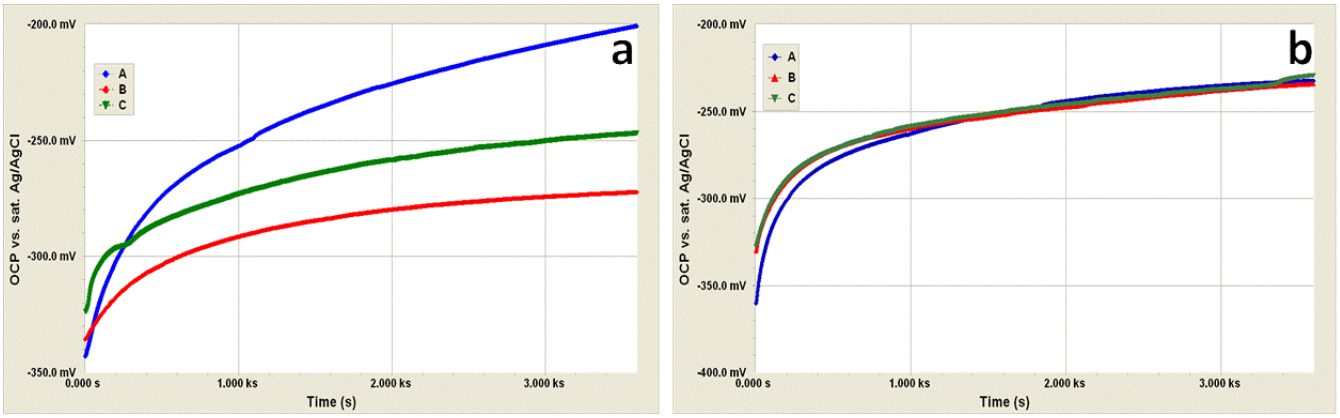

Figure 2. (a) OCP *vs. t* of Fe in 0.3 M $NaHCO_3$ + 0.1 M Na_2CO_3 with smooth surface finish (P1000) (A: 0% Na_2MoO_4, B: 1% Na_2MoO_4, C: 2% Na_2MoO_4). **(b)** OCP *vs. t* of Fe in 0.3 M $NaHCO_3$ + 0.1 M Na_2CO_3 with rough surface finish surface (P120) (A: 0% Na_2MoO_4, B: 1% Na_2MoO_4, C: 2% Na_2MoO_4).

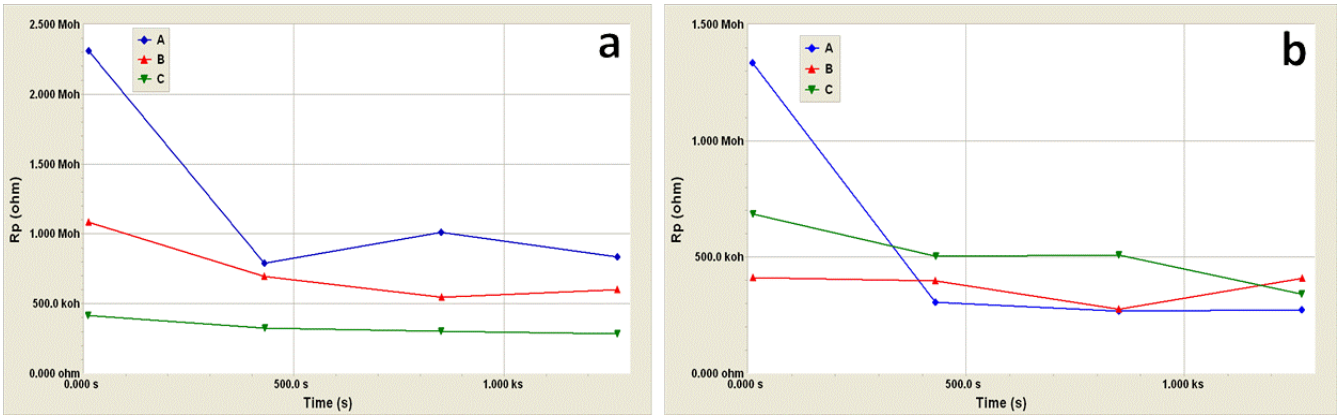

Figure 3. (a) R_p *vs. t* of Fe in 0.3 M $NaHCO_3$ + 0.1 M Na_2CO_3 with smooth surface finish (P1000) (A: 0% Na_2MoO_4, B: 1% Na_2MoO_4, C: 2% Na_2MoO_4). **(b)** R_p *vs. t* of Fe in 0.3 M $NaHCO_3$ + 0.1 M Na_2CO_3 with rough surface finish (P120) (A: 0% Na_2MoO_4, B: 1% Na_2MoO_4, C: 2% Na_2MoO_4)

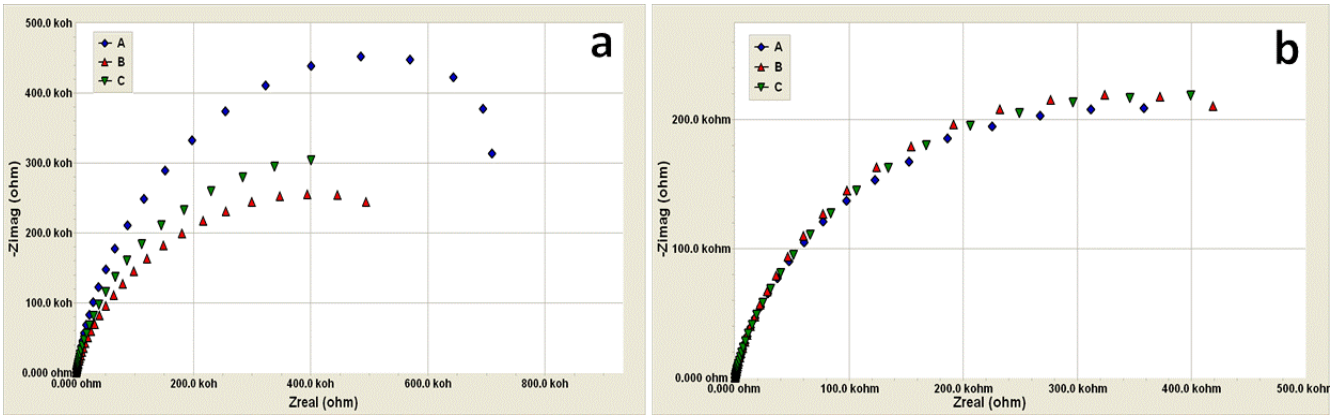

Figure 4. (a) Nyquist plots of Fe in 0.3 M $NaHCO_3$ + 0.1 M Na_2CO_3 with smooth surface finish (P1000) (A: 0% Na_2MoO_4, B: 1% Na_2MoO_4, C: 2% Na_2MoO_4)**. (b)** Nyquist plots of Fe in 0.3 M $NaHCO_3$ + 0.1 M Na_2CO_3 with rough surface finish (P120) (A: 0% Na_2MoO_4, B: 1% Na_2MoO_4, C: 2% Na_2MoO_4).

Table 2a. R_p values of Fe in different solutions in the absence of Cl^- ions extrapolated from the R_p *vs. t* curves.

Solution	R_p (kΩ cm^2)
0.3 M $NaHCO_3$ + 0.1 M Na_2CO_3 (**P1000**)	38.8±19.6
0.3 M $NaHCO_3$ + 0.1 M Na_2CO_3 + 1% Na_2MoO_4 **(P1000)**	22.9±6.62
0.3 M $NaHCO_3$ + 0.1 M Na_2CO_3 + 2% Na_2MoO_4 **(P1000)**	10.4±1.60
0.3 M $NaHCO_3$ + 0.1 M Na_2CO_3 (**P120**)	17.1±14.3
0.3 M $NaHCO_3$ + 0.1 M Na_2CO_3 + 1% Na_2MoO_4 **(P120)**	11.7±1.76
0.3 M $NaHCO_3$ + 0.1 M Na_2CO_3 + 2% Na_2MoO_4 **(P120)**	15.6±3.83

Table 2b. R_p and α values of Fe in different solutions in the absence of Cl^- ions extrapolated from EIS measurements.

Solution	R_p (kΩ cm^2)	α
0.3 M $NaHCO_3$ + 0.1 M Na_2CO_3 (**P1000**)	36.0±0.598	0.8394±0.00127
0.3 M $NaHCO_3$ + 0.1 M Na_2CO_3 + 1% Na_2MoO_4 **(P1000)**	20.5±0.315	0.8167±0.001253
0.3 M $NaHCO_3$ + 0.1 M Na_2CO_3 + 2% Na_2MoO_4 **(P1000)**	30.1±1.06	0.802±0.001335
0.3 M $NaHCO_3$ + 0.1 M Na_2CO_3 (**P120**)	17.7±0.375	0.8136±0.001358
0.3 M $NaHCO_3$ + 0.1 M Na_2CO_3 + 1% Na_2MoO_4 **(P120)**	18.0±0.318	0.8337±0.001295
0.3 M $NaHCO_3$ + 0.1 M Na_2CO_3 + 2% Na_2MoO_4 **(P120)**	17.6±0.346	0.8302±0.001287

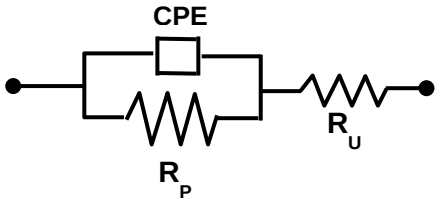

Figure 5. The equivalent circuit used to fit the EIS data. (CPE the constant phase element, R_p the polarization resistance, and the R_u the solution resistance).

CPE is defined by the following equation [24]:

$$Z(\mathrm{CPE}) = Y_0^{-1}(\mathrm{j}\omega)^{-\alpha}$$

in which Y_0 is the CPE constant, ω is the angular frequency in rad s^{-1}, $j^2 = -1$ is the imaginary number, and α is the CPE exponent.

Further inspection of Tables 2a and 2b shows lower R_p values for the rough surfaces when compared to the smooth ones for a given solution. Clearly, the corrosion rate increases with increasing surface roughness. The corrosion current density (i_c) is expressed by $i_c = B/R_p$ where B is a constant represented by $B = \beta_a\beta_c/[2.3(\beta_a+\beta_c)]$ in which β_a and β_c are the anodic and cathodic Tafel slopes extrapolated from the polarization curves, respectively. The physical meaning of the CPE depends on the value of α. CPE represents resistance (Z[CPE] = R, α=0), capacitance (Z[CPE] = C, α=1), inductance (Z[CPE] = L, α=–1), or Warburg impedance for (α = 0.5). The CPE is considered a non-ideal capacitor when values of α are ≥0.8. Generally, deviation from an ideal capacitor (α=1) can be attributed to heterogeneity and roughness. Inspection of Table 2b shows α values greater than 0.8 for both smooth and rough samples. As a result, the CPE can be treated as a non-ideal capacitor in these solutions.

Figure 6(a,b) shows the potentiodynamic polarization curves for Fe as a function of MoO_4^{2-} concentration. Figure 6a represents smooth surface finish while Figure 6b represents rough surface finish. Inspection of the curves in Figure 6 shows a passive region above the E_c. The presence of MoO_4^{2-} resulted in little effect on the passive current densities. Considering all six curves in Figure 6, the passive current densities range from approximately 13 μA cm^{-2} to 32 μA cm^{-2}. Due to such small range, it can be concluded that the presence of MoO_4^{2-} and surface finish (rough *vs.* smooth) do not affect passivity of Fe in these solutions. Figure 7 shows SEM images taken after the potentiodynamic polarization experiments. The images show general corrosion only.

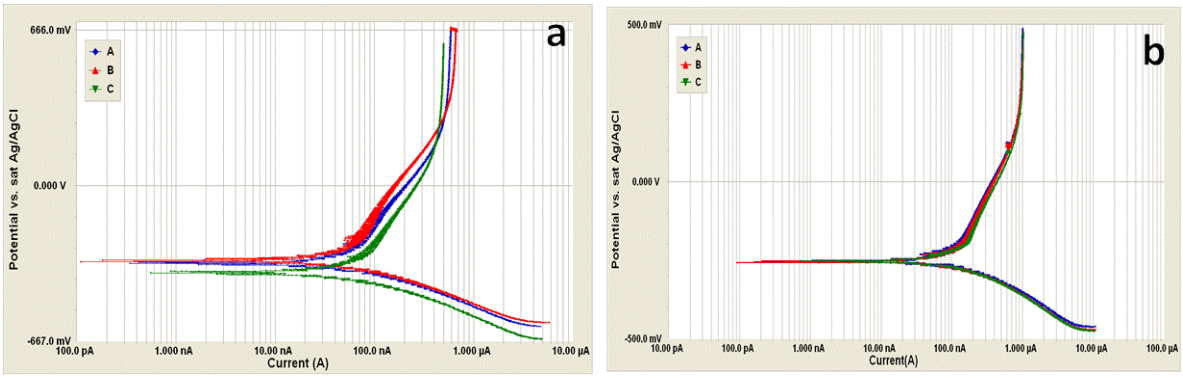

Figure 6. (a) Potentiodynamic polarization curves of Fe in 0.3 M $NaHCO_3$ + 0.1 M Na_2CO_3 with smooth surface finish (P1000) (A: 0% Na_2MoO_4, B: 1% Na_2MoO_4, C: 2% Na_2MoO_4)**. (b)** Potentiodynamic polarization curves of Fe in 0.3 M $NaHCO_3$ + 0.1 M Na_2CO_3 with rough surface finish (P120) (A: 0% Na_2MoO_4, B: 1% Na_2MoO_4, C: 2% Na_2MoO_4).

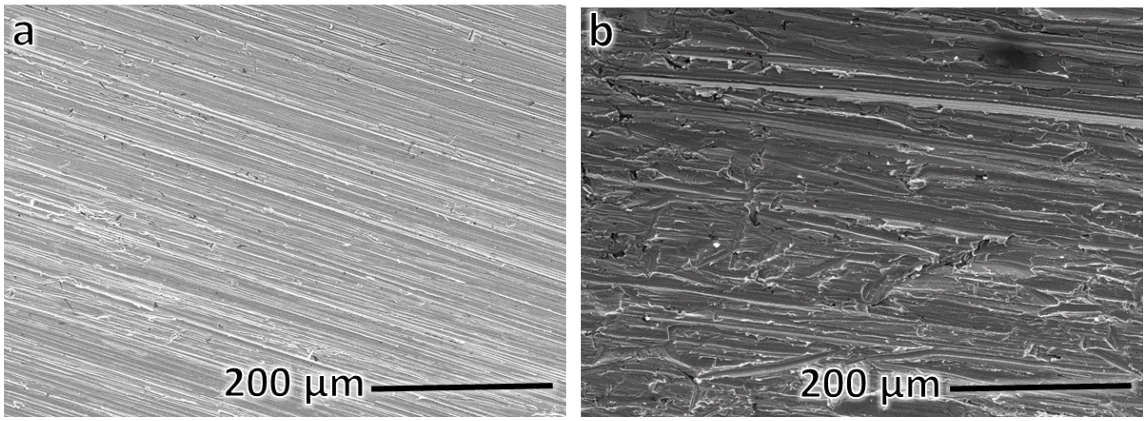

Figure 7. (a) SEM of Fe after potentiodynamic polarization in 0.3 M $NaHCO_3$ + 0.1 M Na_2CO_3 (smooth surface finish P1000). **(b):** SEM of Fe after potentiodynamic polarization in 0.3 M $NaHCO_3$ + 0.1 M Na_2CO_3 (rough surface finish P120).

3.2. The corrosion behavior of Fe in the presence of Cl^- ions

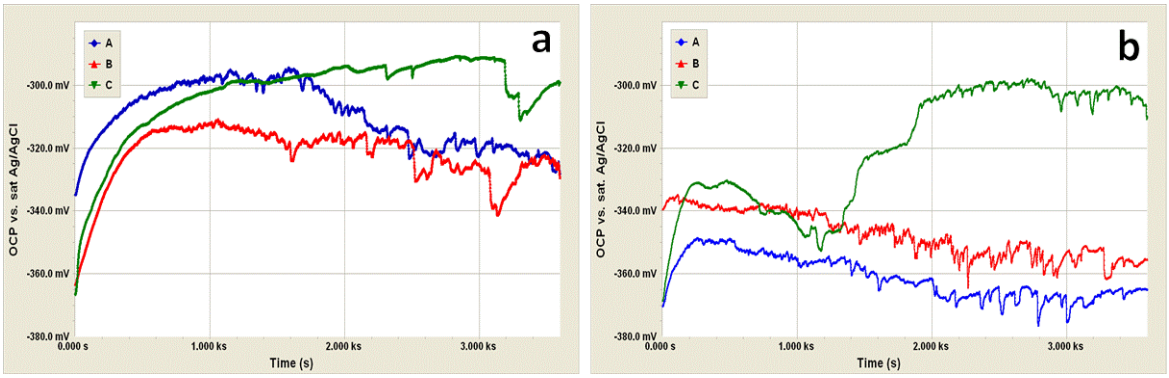

Figure 8. (a) OCP *vs. t* of Fe in 0.3 M $NaHCO_3$ + 0.1 M Na_2CO_3 + 1% NaCl with smooth surface finish (P1000) (A: 0% Na_2MoO_4, B: 1% Na_2MoO_4, C: 2% Na_2MoO_4)**. (b)**: OCP *vs. t* of Fe in 0.3 M $NaHCO_3$ + 0.1 M Na_2CO_3 + 1% NaCl with rough surface finish (P120) (A: 0% Na_2MoO_4, B: 1% Na_2MoO_4, C: 2% Na_2MoO_4).

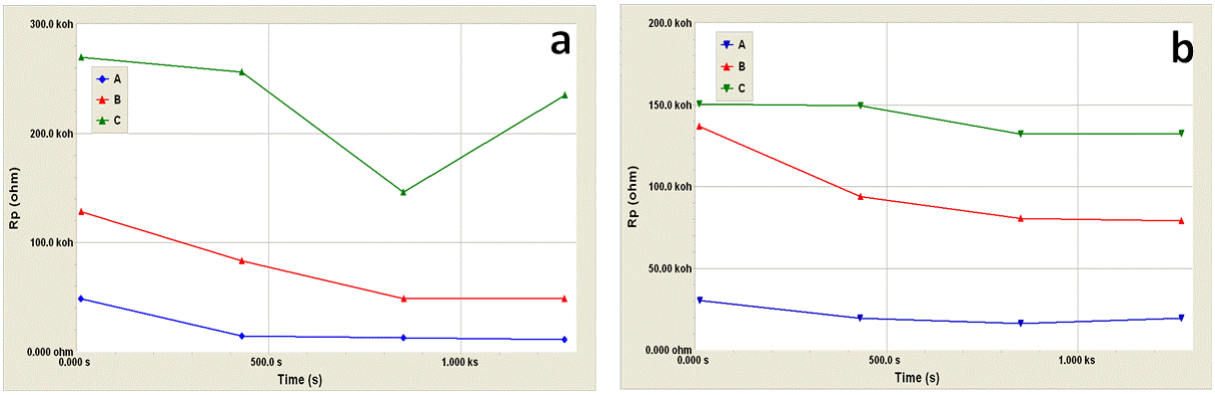

Figure 9. (a): R_p *vs. t* of Fe in 0.3 M $NaHCO_3$ + 0.1 M Na_2CO_3 + 1% NaCl with smooth surface finish (P1000) (A: 0% Na_2MoO_4, B: 1% Na_2MoO_4, C: 2% Na_2MoO_4). **(b)** R_p *vs. t* of Fe in 0.3 M $NaHCO_3$ + 0.1 M Na_2CO_3 + 1% NaCl with rough surface finish (P120) (A: 0% Na_2MoO_4, B: 1% Na_2MoO_4, C: 2% Na_2MoO_4).

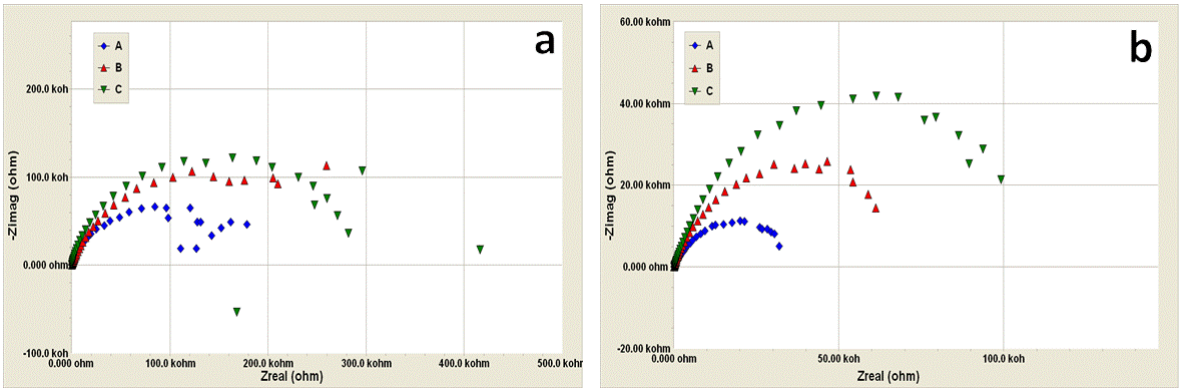

Figure 10. (a) Nyquist plots of Fe in 0.3 M $NaHCO_3$ + 0.1 M Na_2CO_3 + 1% NaCl with smooth surface finish (P1000) (A: 0% Na_2MoO_4, B: 1% Na_2MoO_4, C: 2% Na_2MoO_4). **(b):** Nyquist plots of Fe in 0.3 M $NaHCO_3$ + 0.1 M Na_2CO_3 + 1% NaCl with rough surface finish (P120) (A: 0% Na_2MoO_4, B: 1% Na_2MoO_4, C: 2% Na_2MoO_4).

Figure 8(a,b) shows the OCP *vs. t* for Fe tested in 0.3 M $NaHCO_3$ + 0.1 M Na_2CO_3 + 1% NaCl as a function of MoO_4^{2-} and surface roughness. Figure 8a represents smooth surface finish (P1000) while Figure 8b represents rough surface finish (P120). Inspections of Figures 8a and 8b, the OCP gradually increases before reaching a plateau after few minutes from immersion. Then, the OCP starts to fluctuate combined with an overall decrease in the OCP with time. The latter behavior is especially valid for curves A (0% MoO_4^{2-}) and B (1% MoO_4^{2-}). Curves C (2% MoO_4^{2-}) show less fluctuations in comparison to curves A and B combined with a slight overall increase of the OCP with time. The initial increase in the OCP with time can be attributed to the transformation of the preexisting film to a stable film. However, due to Cl^- attack, the film becomes less stable with the possibility of metastable pits formation as indicated by the OCP fluctuations and its small overall decrease with time. Curves C show less fluctuations, especially for the smooth surface finish samples. The presence of 2% MoO_4^{2-}(curve C) enhances Fe resistance to

corrosion. Figure 9(a,b) shows R_p values *vs. t* curves with the average R_p values reported in Table 3a. Figure 10(a,b) shows the Nyquist plots for the smooth and rough surfaces, respectively. R_p and α values (Table 3b) were obtained by fitting the equivalent electrical circuit (Figure 5) to the impedance data from the EIS measurements. The R_p values extrapolated from the EIS curves and reported in Table 3b follow the same trend of the R_p values extrapolated from R_p *vs*. *t* curves and reported in Table 3a. Examining the R_p values in Tables 2(a,b) and Tables 3(a,b) reveals the following:

1. The R_p values in the presence of Cl^- are lower than the R_p values in the absence of Cl^- for a given solution and surface roughness.
2. In the presence of Cl^-, the smooth surface finish samples have higher R_p values than the rough finish samples.
3. In the presence of Cl^-, the R_p values increase with increasing MoO_4^{2-} concentration.

Table 3a. R_p values of Fe in different solutions in the presence of 1% NaCl extrapolated from the R_p *vs. t* curves.

Solution	R_p (kΩ cm^2)
0.3 M $NaHCO_3$ + 0.1 M Na_2CO_3 + 1% NaCl (**P1000**)	0.683±0.486
0.3 M $NaHCO_3$ + 0.1 M Na_2CO_3 + 1% NaCl + 1% Na_2MoO_4 **(P1000)**	2.43±1.02
0.3 M $NaHCO_3$ + 0.1 M Na_2CO_3 + 1% NaCl + 2% Na_2MoO_4 **(P1000)**	7.12±1.51
0.3 M $NaHCO_3$ + 0.1 M Na_2CO_3 + 1% NaCl (**P120**)	0.673±0.169
0.3 M $NaHCO_3$ + 0.1 M Na_2CO_3 + 1% NaCl + 1% Na_2MoO_4 **(P120)**	3.06±0.735
0.3 M $NaHCO_3$ + 0.1 M Na_2CO_3 + 1% NaCl + 2% Na_2MoO_4 **(P120)**	4.43±0.278

Table 3b. R_p and α values of Fe in different solutions in the presence of 1% NaCl extrapolated from EIS measurements.

Solution	R_p (kΩ cm^2)	α
0.3 M $NaHCO_3$ + 0.1 M Na_2CO_3 + 1% NaCl (**P1000**)	4.89±0.0435	0.8365±0.001513
0.3 M $NaHCO_3$ + 0.1 M Na_2CO_3 + 1% NaCl + 1% Na_2MoO_4 **(P1000)**	9.73±0.149	0.7856±0.001318
0.3 M $NaHCO_3$ + 0.1 M Na_2CO_3 + 1% NaCl + 2% Na_2MoO_4 **(P1000)**	8.37±.07056	0.9005±0.001417
0.3 M $NaHCO_3$ + 0.1 M Na_2CO_3 + 1% NaCl (**P120**)	1.15±0.01551	0.6951±0.001675
0.3 M $NaHCO_3$ + 0.1 M Na_2CO_3 + 1% NaCl + 1% Na_2MoO_4 **(P120)**	2.38±0.03162	0.7426±0.001563
0.3 M $NaHCO_3$ + 0.1 M Na_2CO_3 + 1% NaCl + 2% Na_2MoO_4 **(P120)**	3.71±0.04581	0.7638±0.00143

Clearly, while the presence of Cl^- ions increased the corrosion rate of Fe, the addition of MoO_4^{2-} enhanced the corrosion resistance of Fe in bicarbonate/carbonate solutions containing Cl^-. Inspection of the α values reported in Table 3b shows a range from 0.6951 to 0.9005. Moreover, the lowest α values were obtained for the rough surfaces. Cl^- is known to induce localized (pitting) corrosion. The lowest reported value for all solutions (α = 0.6951) is obtained for a rough surface in the presence of Cl^- and in the absence of MoO_4^{2-}. Pitting corrosion is expected to occur under these conditions. As a result, CPE cannot be treated as a capacitor.

Figure 11(a,b) shows the potentiodynamic polarization curves for Fe in 0.3 M $NaHCO_3$ + 0.1 M Na_2CO_3 + 1% NaCl as a function of MoO_4^{2-} and surface roughness. Comparing curves A in Figure 11 (presence of Cl^-) to curves A in Figure 6 (absence of Cl^-) shows that the presence of Cl^- resulted in passivity breakdown at about –200 mV (pitting potential). Comparing curve A in Figure 11a (smooth) to curve A in Figure 11b (rough) reveals the rough surface resulted in smaller passive potential range in comparison to the smooth surface. The presence of MoO_4^{2-} resulted in increasing the passive potential range, lower passive current densities, and higher pitting potentials as seen in curves B and C in Figure 11. Figure 12 shows SEM images of Fe surfaces under different conditions. Figures 12(a) and 12(b) show Fe with rough surface finish after one hour of immersion (at OCP) in 0.3 M $NaHCO_3$ + 0.1 M Na_2CO_3 + 1% NaCl in the absence and presence of 2% Na_2MoO_4, respectively. Figures 12(c) and 12(d) show Fe with rough surface finish after 72 hours of immersion. The images show general corrosion only with no signs of pitting corrosion. Figures 12(e) and 12(f) show SEM images of Fe in 0.3 M $NaHCO_3$ + 0.1 M Na_2CO_3 + 1% NaCl in the absence of MoO_4^{2-}. Figures 12(g) and 12(h) show SEM images of Fe in 0.3 M $NaHCO_3$ + 0.1 M Na_2CO_3 + 1% NaCl in the presence of 1% MoO_4^{2-}. Figures 12(i) and 12(j) show SEM images of Fe in 0.3 M $NaHCO_3$ + 0.1 M Na_2CO_3 + 1% NaCl in the presence of 2% MoO_4^{2-}. The SEM images were taken after the potentiodynamic polarization experiments. While the presence of 1% NaCl resulted in pitting corrosion in the absence of MoO_4^{2-} and in the presence of 1% MoO_4^{2-}, the presence of 2% MoO_4^{2-} inhibited pitting corrosion. Based on the potentiodynamic polarization experiments and SEM images, the presence of sufficient concentration of MoO_4^{2-} enhances the pitting corrosion resistance of Fe in the presence of Cl^- by increasing the pitting potential and decreasing the passive current densities.

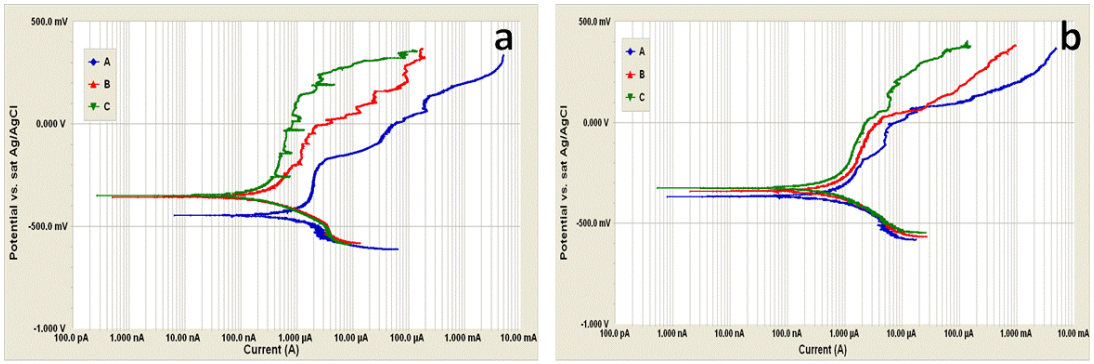

Figure 11. (a) Potentiodynamic polarization curves of Fe in 0.3 M $NaHCO_3$ + 0.1 M Na_2CO_3 + 1% NaCl with smooth surface finish (P1000) (A: 0% Na_2MoO_4, B: 1% Na_2MoO_4, C: 2% Na_2MoO_4). **(b)** Potentiodynamic polarization curves of Fe in 0.3 M $NaHCO_3$ + 0.1 M Na_2CO_3 + 1% NaCl with rough surface finish (P120) (A: 0% Na_2MoO_4, B: 1% Na_2MoO_4, C: 2% Na_2MoO_4).

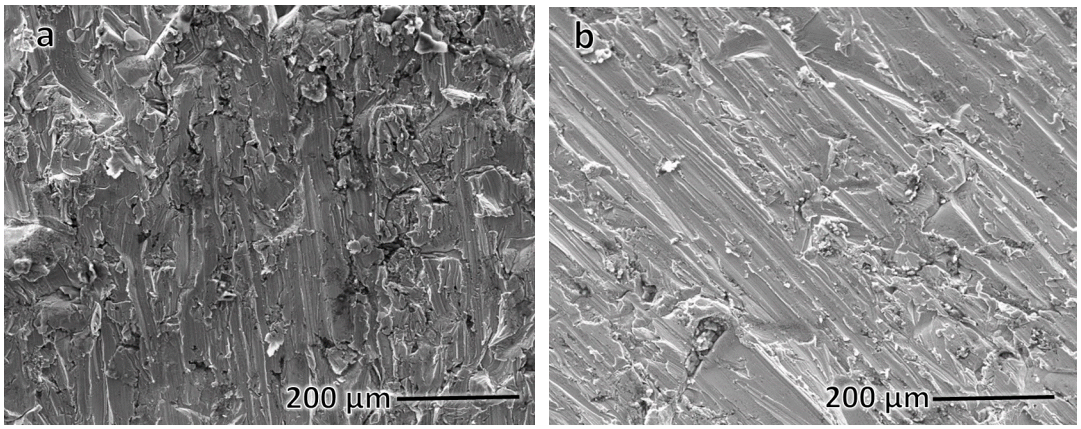

Figure 12. (a): SEM of Fe after one hour of immersion in 0.3 M $NaHCO_3$ + 0.1 M Na_2CO_3 + 1% NaCl (rough surface finish P120). **(b):** SEM of Fe after one hour of immersion at the OCP in 0.3 M $NaHCO_3$ + 0.1 M Na_2CO_3 + 1% NaCl + 2% Na_2MoO_4 (rough surface finish P120).

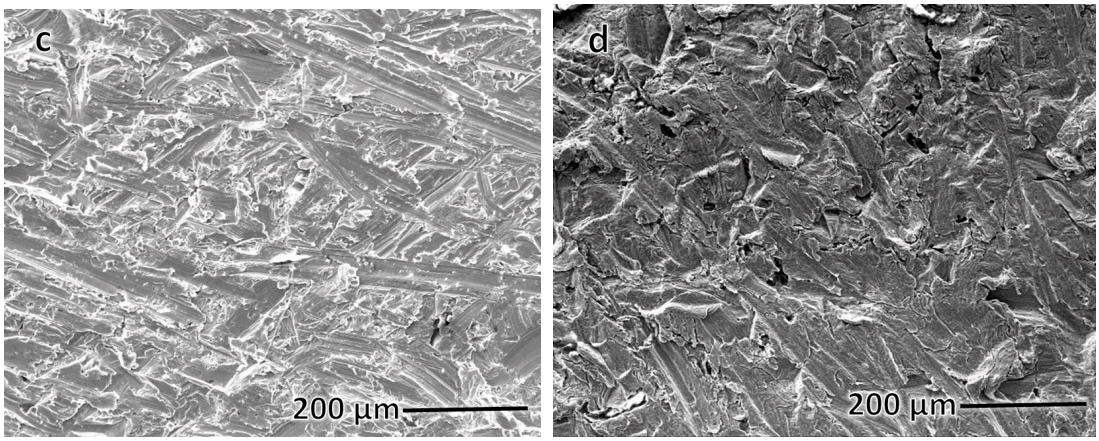

Figure 12. (c): SEM of Fe after 72 hours of immersion in 0.3 M $NaHCO_3$ + 0.1 M Na_2CO_3 + 1% NaCl (rough surface finish P120). **(d):** SEM of Fe after 72 hours of immersion at the OCP in 0.3 M $NaHCO_3$ + 0.1 M Na_2CO_3 + 1% NaCl + 2% Na_2MoO_4 (rough surface finish P120).

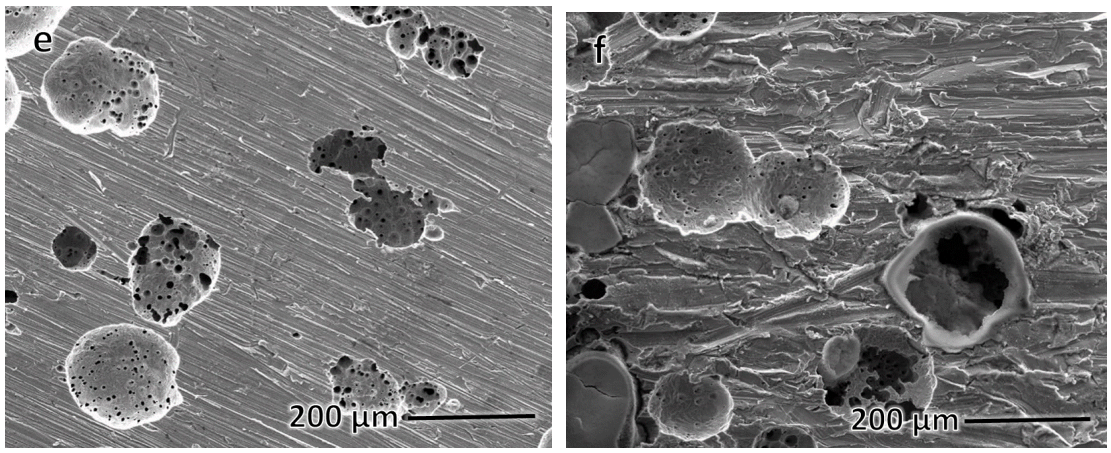

Figure 12. (e): SEM of Fe after potentiodynamic polarization in 0.3 M $NaHCO_3$ + 0.1 M Na_2CO_3 + 1% NaCl (smooth surface finish P1000). **(f):** SEM of Fe after potentiodynamic polarization in 0.3 M $NaHCO_3$ + 0.1 M Na_2CO_3 + 1% NaCl (rough surface finish P120)

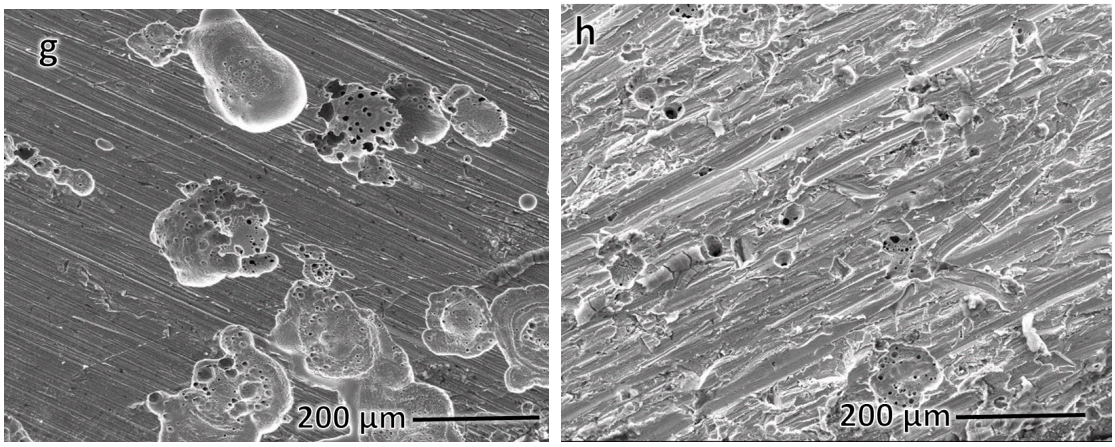

Figure 12. (g): SEM of Fe after potentiodynamic polarization in 0.3 M $NaHCO_3$ + 0.1 M Na_2CO_3 + 1% NaCl + 1% Na_2MoO_4 (smooth surface finish P1000). **(h):** SEM of Fe after potentiodynamic polarization in 0.3 M $NaHCO_3$ + 0.1 M Na_2CO_3 + 1% NaCl + 1% Na_2MoO_4 (rough surface finish P120).

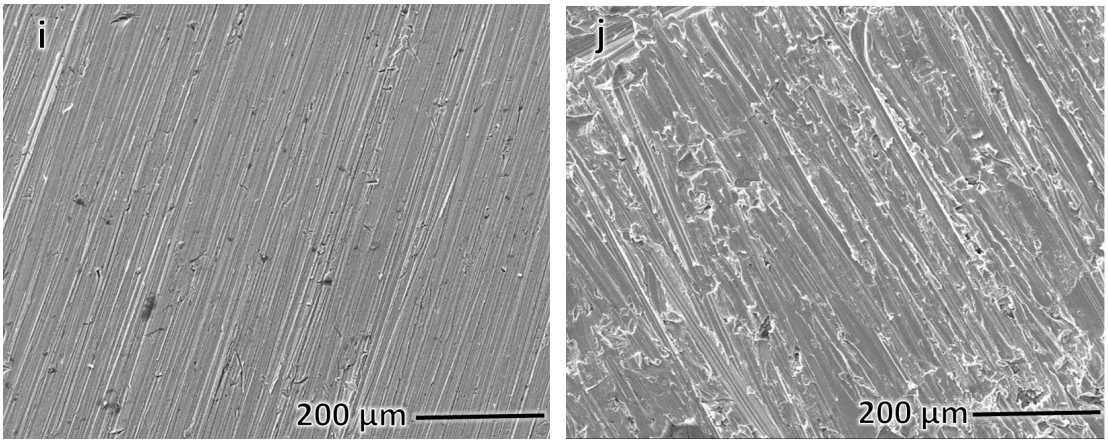

Figure 12. (i): SEM of Fe after potentiodynamic polarization in 0.3 M $NaHCO_3$ + 0.1 M Na_2CO_3 + 1% NaCl + 2% Na_2MoO_4 (smooth surface finish P1000). **(j):** SEM of Fe after potentiodynamic polarization in 0.3 M $NaHCO_3$ + 0.1 M Na_2CO_3 + 1% NaCl + 2% Na_2MoO_4 (rough surface finish P120).

Conclusions

4.1. In the absence of Cl^-:

1. The presence of MoO_4^{2-} does not enhance the corrosion resistance of Fe in 0.3 M $NaHCO_3$ + 0.1 M Na_2CO_3. Interestingly, small concentrations of MoO_4^{2-} might decrease the corrosion resistance. This is true for smooth and rough surface finishes.
2. MoO_4^{2-} and surface finish do not affect passivity of Fe in 0.3 M $NaHCO_3$ + 0.1 M Na_2CO_3.
3. The CPE can be treated as a non-ideal capacitor in 0.3 M $NaHCO_3$ + 0.1 M Na_2CO_3 in the absence and presence of MoO_4^{2-}. This is true for smooth and rough surface finishes.

4.2. In the presence of Cl^- ions:

1. The presence of Cl^- increases the corrosion rate of Fe in 0.3 M $NaHCO_3$ + 0.1 M Na_2CO_3.
2. The smooth finish surfaces have lower corrosion rates than the rough finish surfaces for a given solution.
3. The corrosion rate decreases with increasing MoO_4^{2-} concentration.
4. The CPE *can* be treated as a non-ideal capacitor in 0.3 M $NaHCO_3$ + 0.1 M Na_2CO_3 + 1% NaCl in the absence and presence of MoO_4^{2-} for the relatively smooth finish surface but not the relatively rough surface finish where α is less than 0.80.
5. The presence of MoO_4^{2-} enhances the pitting corrosion resistance of Fe in 0.3 M $NaHCO_3$ + 0.1 M Na_2CO_3 + 1% NaCl by increasing the pitting potential and decreasing the passive current densities.

Acknowledgment

The authors would like to express their sincere appreciation to the Research Affairs at the United Arab Emirates University (UAEU) for their partial support of this project under SURE + 2019. The authors would also like to express their gratitude to the department of chemistry at the UAEU for providing the facilities to carry out this project. The authors would like to thank Professor Nathir Alrawashdeh from the Higher Colleges of Technologies (HCT) for his help with the manuscript.

References

1. J. Soltis, *Corros. Sci*., 2015, **90**, no. 1, 5–22. doi: 10.1016/j.corsci.2014.10.006
2. A. Veluchamy, D. Sherwood, B. Emmanuel and I.S. Cole, *J. Electroanal. Chem*., 2017, **785**, 196–215. doi: 10.1016/j.jelechem.2016.12.020
3. M. Moreno, W. Morris, M.G. Alvarez and G.S. Duffo, *Corros. Sci*., 2004, **46**, no. 11, 2681–2699. doi: 10.1016/j.corsci.2004.03.013
4. Y.T. Tan, S.L. Wijesinghe and D.J. Blackwood, *Corros. Sci*., 2014, **88**, 152–160. doi: 10.1016/j.corsci.2014.07.026

5. N.N. Andreev, I.A. Gedvillo, A.S. Zhmakina, D.S. Bulgakov and S.S. Vesely, *Int. J. Corros. Scale Inhib.*, 2016, **5**, no. 4, 319–324. doi: 10.17675/2305-6894-2016-5-4-2
6. I.A. Gedvillo, A.S. Zhmakina, N.N. Andreev and S.S. Vesely, *Int. J. Corros. Scale Inhib.*, 2017, **6**, no. 1, 82–90. doi: 10.17675/2305-6894-2017-6-1-7
7. V.S. Sastri, *Green Corrosion Inhibitors*, John Wiley and Sons, New Jersey, 2011, ISBN 978-0-470-45210-3.
8. J.R. Ambrose, *Corrosion*, 1978, **34**, no. 1, 27–31. doi: 10.5006/0010-9312-34.1.27
9. T. Kodama and J.R. Ambrose, *Corrosion*, 1977, **33**, no. 5, 155–161. doi: 10.5006/0010-9312-33.5.155
10. K. Sugimoto and Y. Sawada, *Corrosion*, 1976, **32**, no. 9, 347–352. doi: 10.5006/0010-9312-32.9.347
11. C.R. Clayton and Y.C. Lu, *Corros. Sci.*, 1989, **29**, no. 7, 881–898. doi: 10.1016/0010-938x(89)90059-0
12. S. Virtanen, B. Surber and P. Nylund, *Corros. Sci.*, 2001, **43**, no. 6, 1165–1177. doi: 10.1016/s0010-938x(00)00121-9
13. A.S. Alshamsi, *Int. J. Basic Appl. Sci.*, 2013, **2**, no. 4, 303–311. doi: 10.14419/ijbas.v2i4.1129
14. S.A.M. Refaey, *Appl. Surf. Sci.*, 2005, **240**, no. 1–4, 396–404. doi: 10.1016/j.apsusc.2004.07.014
15. X. Li, S. Deng and H. Fu, *Corros. Sci.*, 2011, **53**, no. 9, 2748–2753. doi: 10.1016/j.corsci.2011.05.002
16. M.R. Ali, C.M. Mustafa and M. Habib, *J. Sci. Res. (Rajshahi, Bangladesh)*, 2009, **1**, no. 1, 82. doi: 10.3329/jsr.v1i1.1053
17. A.S. Alshamsi, *Int. J. Electrochem. Sci.*, 2013, **8**, no. 1, 591–605.
18. A.S. Alshamsi and A. AlBlooshi, *Int. J. Electrochem. Sci.*, 2019, **14**, no. 6, 5794–5812. doi: 10.20964/2019.06.64
19. Y.T. Tan, S.L. Wijesinghe and D.J. Blackwood, *J. Electrochem. Soc.*, 2017, **164**, no. 9, C505-C515. doi: 10.1149/2.0501709jes
20. G.O. Ilevbare and G.T. Burstein, *Corros. Sci.*, 2003, **45**, 1545. doi: 10.1016/s0010-938x(02)00229-9
21. D. Dwivedi, K. Lepkova and T. Becker, *RSC Adv.*, 2017, **7**, no. 8, 4580–4610. doi: 10.1039/c6ra25094g
22. G.T. Burstein and P.C. Pistorius, *Corrosion*, 1995, **51**, no. 5, 380–385. doi: 10.5006/1.3293603
23. H. Wang, Y. Li, G. Cheng, W. Wu, Y. Zhang and X. Li, *Int. J. Electrochem. Sci.*, 2018, **13**, no. 5, 5268–5283. doi: 10.20964/2018.06.05
24. Z. Zhang, S. Chen, Y. Li, S. Li and L. Wang, *Corros. Sci.*, 2009, **51**, no. 2, 291–300. doi: 10.1016/j.corsci.2008.10.040

♦ ♦ ♦